NOTE / NOTE

Characterization of the ATP-translocating properties of the predicted *Arabidopsis thaliana* mitochondrial adenine nucleotide translocator 2

Olesya A. Kharenko and Michele C. Loewen

Abstract: In this study we demonstrate that the predicted *Arabidopsis thaliana* (L.) Heynh. mitochondrial adenine nucleotide translocator 2 (ANT2) mediates ATP translocation. The demonstration that recombinantly produced ANT2 mediates ATP uptake into proteoliposomes, confirms previous sequence-based identification of the protein as a member of the adenine nucleotide translocator family. Expressed in *Saccharomyces cerevisiae* with a C-terminal His6 tag, localization was confirmed in yeast membrane extracts. The recombinant protein was solubilized with Triton X-100, enriched by immobilized metal affinity chromatography, and reconstituted into liposomes. Functionality of the reconstituted protein was confirmed by demonstration of pyridoxal 5′-phosphate-sensitive [^{3}H]ATP uptake. Transport assays showed first order kinetic uptake of ATP with an approximate K_m value of 15 μmol·L^{-1}. Competition assays indicated that the reconstituted protein had highest specificity for ATP. Overall, these results indicate that *Arabidopsis* ANT2 is an adenine nucleotide translocator.

Key words: adenine nucleotide translocator 2, *Arabidopsis thaliana*, functional characterization, mitochondria, recombinant expression.

Résumé : Dans cette étude, les auteurs démontrent leur prédiction à l'effet que le transporteur du nucléotide adénine (ANT2) mitochondrial intervient dans le transport de l'ATP. Que l'ANT2 produit par recombinaison intervienne dans l'absorption de l'ATP dans des protéoliposomes confirme l'identification basée sur les séquences de la protéine comme membre de la famille des transporteurs du nucléotide adénine. Les auteurs confirment sa présence dans des extraits de membranes de levure, lorsqu'on l'exprime chez le *Saccharomyces cerevisiae*, avec un marqueur C-terminal His6. On a solubilizé la protéine recombinante avec du Triton X-100 et on l'a enrichie par chromatographie d'affinité sur métal immobilisé, avant de la reconstituer dans des liposomes. Les auteurs ont ainsi confirmé la fonctionnalité de la protéine reconstituée en démontrant l'absorption du pyridoxal 5′ [^{3}H]ATP sensible au phosphate. Des essais de transport montrent une absorption cinétique de premier ordre de l'ATP, avec une valeur K_m approximative de 15 μmol·L^{-1}. Les essais de compétition indiquent que la protéine reconstituée possède une plus grande affinité pour l'ATP. En général, ces résultats montrent que l'ANT2 de l'*Arabidopsis* constitue un transporteur du nucléotide adénine.

Mots-clés : transporteur 2 du nucléotide adénine, *Arabidopsis thaliana*, caractérisation fonctionnelle, mitochondrie, expression de recombinaison.

[Traduit par la Rédaction]

Introduction

Adenine nucleotide translocators (ANTs) are a family of proteins that play a major role in energy metabolism, catalyzing ATP/ADP exchange across membranes (Kunji 2004). In plants, different ANTs are localized to the inner membranes of the endoplasmic reticulum, mitochondria, and chloroplasts (Millar and Heazlewood 2003; Leroch et al. 2008). Various physiological processes and metabolic pathways are strictly dependent on the ATP pools available and decrease of ANT activity can lead to complete inhibition of cellular metabolism (Neuhaus et al. 1997; Klingenberg 2008). This makes ANT activity essential to cellular growth and development.

Arabidopsis thaliana (L.) Heynh. is a known plant model system, the genome of which has been completely sequenced (Picault et al. 2004). To date, one endoplasmic reticulum (ER-ANT1), two plastidic (At1g80300 and At1g15500), and at least three mitochondrial [At5g13490

Received 16 December 2009. Accepted 21 April 2010. Published on the NRC Research Press Web site at botany.nrc.ca on 2 July 2010.

O.A. Kharenko and M.C. Loewen.[1] Plant Biotechnology Institute, National Research Council of Canada, 110 Gymnasium Place, Saskatoon, SK S7N 0W9, Canada.

[1]Corresponding author (e-mail: Michele.Loewen@nrc-cnrc.gc.ca).

(ANT2), At3g8580 (ANT1), and At4g01100 (ADNT1)] ANTs have been identified (Neuhaus et al. 1997; Klingenberg 2008; Palmieri et al. 2008). While the plastidic ANTs from *A. thaliana* have been extensively studied, their structures are not homologous to, and their biochemical function differs from, the mitochondrial ANTs (Knirsch et al. 1989; Schünemann et al. 1993; Brustovetsky and Klingenberg 1994; Mozo et al. 1995; Genchi et al. 1996; Fiore et al. 1998; Möhlmann et al. 1998; Tjaden et al. 1998; Trentmann et al. 2000; Leroch et al. 2008). ER-ANT1 is unique in its localization and has also been fairly well characterized (Leroch et al. 2008). In the case of mitochondrial ANTs, ADNT1 has been reasonably well characterized, but it shows no homology to any other known ANTs and in-planta studies indicate tissue expression is limited to root tips (Palmieri et al. 2008). Finally, while mitochondrial ANT1 and ANT2 are predicted to be ANTs based on sequence, the proteins themselves have not been isolated and ATP-translocating properties have not been characterized (Schuster et al. 1993; Klingenberg 2008).

In this note, the ATP-translocating functionality of a recombinantly expressed version of *Arabidopsis* ANT2 is demonstrated. Specifically, a C-terminally His-tagged fusion ANT2 protein was expressed in *Saccharomyces cerevisiae*, solubilized in Triton X-100 detergent, and enriched by immobilized metal affinity chromatography. Reconstitution into liposomes yielded a functional ATP-translocator. Kinetic analyses highlighted first-order kinetics of ATP-uptake with an apparent K_m of 15 μmol·L^{-1} and V_{max} of 45 μmol^{-1}·min^{-1}·(g protein)$^{-1}$. Competition studies on recombinant ANT2 indicated sensitivity to the known translocator inhibitor, pyridoxal 5′-phophate, and demonstrated its specificity for ATP and ADP. Overall, these studies demonstrate the ATP-translocating functionality of ANT2, and confirm its identity as an adenine nucleotide translocator.

Methods and materials

Materials

All chemicals were obtained from Sigma-Aldrich (Oakville, Ontario) unless otherwise stated in the text.

Cloning and expression of ANT2

Maximal expression for the At5g13490 (ATP/ADP-Carrier Protein) gene occurs at a stage in development just prior to growth of the first flowering bud, shortly after 20 d post germination in the *A. thalinana* life cycle (data available at www.genevestigator.com/gv/index.jsp). Therefore, using the PolyATract System1000 kit (Promega, Madison, Wisconsin), total RNA was isolated from 23-day-old seedlings of *A. thaliana* ('Columbia' ecotype). The integrity of RNA was confirmed by 1% non-denaturing agarose gel electrophoresis. The mRNA was extracted from the total RNA using MagneSphere Magnetic Separation Products (Promega, Madison, Wisc.), and subsequently reverse-transcribed with the *C. therm* Polymerase One Step RT-PCR System Kit (Roche, Mississauga, Ont.), according to manufacturers' recommendations. PCR primers (forward 5′-GGAATCATATGGTTGAACAGACTCAGCACCCC-3′ and reverse 5′-GCACCTCCAGATCCATACTTCTTGCC-3′) were based on the genomic sequence described (Schuster et al. 1993). The amplified PCR product was sequenced and subsequently cloned into the pYES2.1/V5-His-Topo yeast expression vector (Invitrogen, Carlsbad, California) as a fusion protein with the carboxy terminal V5-epitope and His6 tags. In this vector, the cDNA is expressed under the control of the galactose inducible yeast *GAL1* promoter. The recombinant vector was transformed into Top10 *E. coli* (Invitrogen), screened for the inserts and sequenced.

The chosen pYES2.1/V5-His-Topo cloned construct was transformed into *S. cerevisiae*. Protein expression was induced by transferring the growing yeast culture from a SC-U – 2% glucose based media (Invitrogen) to YPD – 2% galactose based media (Sigma-Aldrich / Becton Dickinson and Company, Mississauga, Ont.). All cultures were grown at 30 °C. Induction proceeded for 7 h prior to harvesting the cells by centrifugation at 4 °C and 4000*g* for 30 min. The cell pellet was resuspended in 50 mmol·L^{-1} phosphate – 300 mmol·(L NaCl buffer)$^{-1}$ (pH 8) containing 5% glycerol, 5 mmol·(L 2-mercaptoethanol)$^{-1}$, and 1 mmol·(L phenylmethylsulphonyl fluoride)$^{-1}$ (PMSF). The resuspended samples were kept on ice and used the same day.

Saccharomyces cerevisiae cells, containing the pYES2.1/V5-His-Topo (Invitrogen) yeast expression vector with no DNA insert, were treated as described above to obtain cell extracts for use as negative controls in SDS–PAGE and Western blot expression analyses. The identification of visualized proteins was carried out by submission of excised bands from silver stained SDS–PAGE for mass spectroscopic based peptide mass fingerprinting analysis at the Mass Spectroscopy facility of the National Research Council – Plant Biotechnology Institute.

Preparation of *Saccharomyces cerevisiae* soluble and membrane fractions

The resuspended *S. cerevisiae* cell pellet was subjected to French Press set at 2000 psi (1 psi = 6.895 kPa) , and then centrifuged at 1500*g*. The supernatant was transferred to Beckman ultra-clear centrifuge tubes and centrifuged at 50 000*g* for 1 h at 4 °C. The resulting supernatant was set aside as the soluble protein fraction. The resulting pellet, containing the membrane fractions, was resuspended in lysis buffer (50 mmol·(L phosphate)$^{-1}$ – 300 mmol·(L NaCl buffer)$^{-1}$ (pH 8), 5% glycerol, 5 mmol·(L 2-mercaptoethanol)$^{-1}$, and 1 mmol·(L PMSF)$^{-1}$) and sonicated for 1 min on ice.

Affinity-based enrichment of recombinant ANT2

Lysis of the resuspended *S. cerevisiae* cell pellets was performed using a French Press set at 1500 psi. The lysate was solubilized by stirring in 50 mmol·(L phosphate)$^{-1}$ – 300 mmol·(L NaCl buffer)$^{-1}$ at pH 8 containing 5% glycerol and 3% Triton X-100. After 1 h, the mixture was centrifuged at 4000*g*. The supernatant was applied to a Ni-NTA column, washed and eluted with imidizole, according to manufacturer's instructions (QIAGEN, Mississauga, Ont.). Concentration of the eluted protein was estimated using an SPN-protein assay (Genotech, St. Louis, Missouri). Samples were tested for enrichment of recombinant ANT2 protein by SDS–PAGE on 10% acrylamide gels and Western blot detection using anti-V5-HRP antibody as the primary antibody with detection by chemiluminescence.

Reconstitution of purified ANT2 into liposomes

Immediately following protein purification, liposomes were prepared by sonication of 100 mg·(mL phosphatidylcholine)$^{-1}$ from egg yolks (Avanti Polar Lipids, Alabaster, Alabama) in 20 mmol·(L NaCl)$^{-1}$ / 10 mmol·(L piperazine-N,N′-bis(2-ethanesulfonic acid) buffer)$^{-1}$ (PIPES, pH 7) containing 1 mmol·(L EDTA)$^{-1}$, 3% cholesterol (*w*/*v*) and 20 mmol·(L ATP)$^{-1}$. Sonication was performed on ice using a Branson sonicator with a microtip (standard HS-200 probe, Mandel Scientific, Guelph, Ont.) for 1 h with 20 s sonication and 20 s intermission intervals.

The recombinant ANT2 protein was incorporated into the liposomes by a freeze–thaw procedure (Bisaccia et al. 1985). Sonicated liposomes were mixed with the His6 affinity-purified solubilized protein (final protein concentration of 10 mg·mL^{-1}). After 15 min incubation on ice, the mixture was frozen in liquid nitrogen. The proteoliposomes were thawed at room temperature and pulse-sonicated for 6 s (0.3 s sonication, 0.7 s intermission) on ice. After sonication, the mixture was passed 15 times through an Amberlite XAD-2 column (Supelco, Oakville, Ont.), pre-equilibrated with 10 mmol·(L PIPES)$^{-1}$ (pH 7) and 20 mmol·(L ATP)$^{-1}$, to remove excess detergent. External ATP was removed by passing the proteoliposomes through G-25, P10 columns (PD-10 Amersham Biosciences, Baie D'Urfe, Quebec), pre-equilibrated with 10 mmol·(L PIPES)$^{-1}$ – 50 mmol·(L NaCl buffer)$^{-1}$ (pH 7) and eluted with the same buffer according to manufacturer's recommendations.

ATP-transport assays

The proteoliposomes were distributed as 25 µL samples into Eppendorf tubes and equilibrated to room temperature for the subsequent transport reactions. At $t = 0$, [^{3}H]ATP was added at the indicated concentrations. After the desired time interval (see below), 2 mmol·(L pyridoxal 5′-phosphate)$^{-1}$ was added as an inhibitor of translocation and 10 µL of the reaction mixtures were transferred to SPN columns. Residual external radioactivity was removed by washing the columns twice with 100 µL of cold (–20 °C) Orgo-Sol™ buffer (Genotech). The filters were separated from the columns and transferred into scintillation vials containing 4 mL scintillation fluid. Bound radioactivity was measured using a Beckman Coulter multi-purpose scintillation counter. Non-specific binding to liposomes and filters was accounted for by subtracting from the experimental values, values derived under the same conditions, but with the addition of 2.0 mmol·(L pyridoxal 5′-phosphate)$^{-1}$ (inhibitor) prior to addition of the [^{3}H] ATP. As an alternative control for non-specific binding, [^{3}H]ATP-uptake into liposomes containing no ANT2 was also determined at various time points following addition of inhibitor after the designated time interval as described above. For kinetic analyses, rates of ATP uptake were determined for each concentration point by completion of a full time-course analysis (including 0, 1, 2.5, 5, and 10 min time points). Each resulting time course curve was fitted to first order kinetics using Origin software (OriginLab, Northampton, Massachusetts) from which a rate was obtained for the given concentration of ATP. Kinetic values were obtained from these rates by Michaelis–Menten analysis using ENZFITTER software (Biosoft, Cambridge, UK).

Fig. 1. Expression and liposome reconstitution of recombinant ANT2. Upper panel: Expression of ANT2 fusion protein as detected by Western blot using an anti-V5 epitope antibody. Lane 1, supernatant; Lane 2, membrane fraction from pYES2.1/V5-His-Topo ANT2 expressing *S. cerevisiae*. Lower Panels: Confirmation of the reconstitution of enriched ANT2 fusion protein. Left, SDS–PAGE stained with Coomassie Blue dye. Right, Western blot Detection using Anti-V5-Epitope-HRP antibody. Lane 1, Triton X-100 solubilized total yeast cell extract; Lane 2, liposome reconstituted purified ANT2 fusion protein.

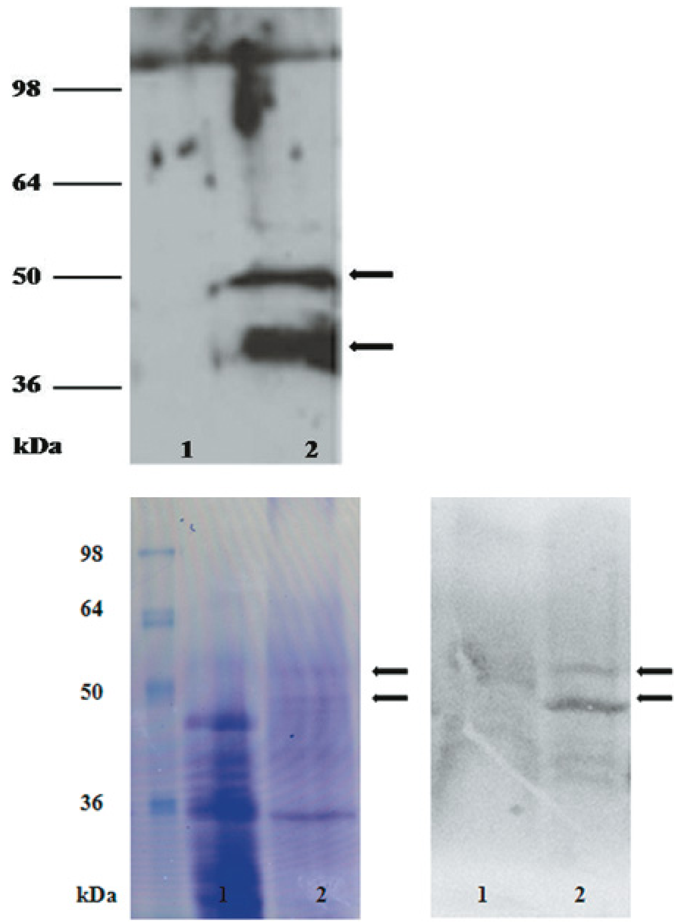

Results

Expression purification and liposome reconstitution of recombinant ANT2

The cDNA encoding ANT2 was ligated into the yeast expression vector pYES2.1 (Invitrogen) in frame with C-terminal His6 and V5-epitope tags and resulting construct transformed into *S. cerevisiae* for expression of the ANT2 fusion protein. Cells were harvested 7 h after galactose induction. The presence of ANT2 fusion protein was detected by Western blot, using an anti-V5-HRP antibody (Fig. 1, top panel). Two bands were detected in the membrane fraction, one at 42 kDa, as expected, based on the calculated molecular weight of the fusion protein, and a second at 48 kDa. ANT2 was not detected in the soluble fraction. The corresponding bands were excised from sil-

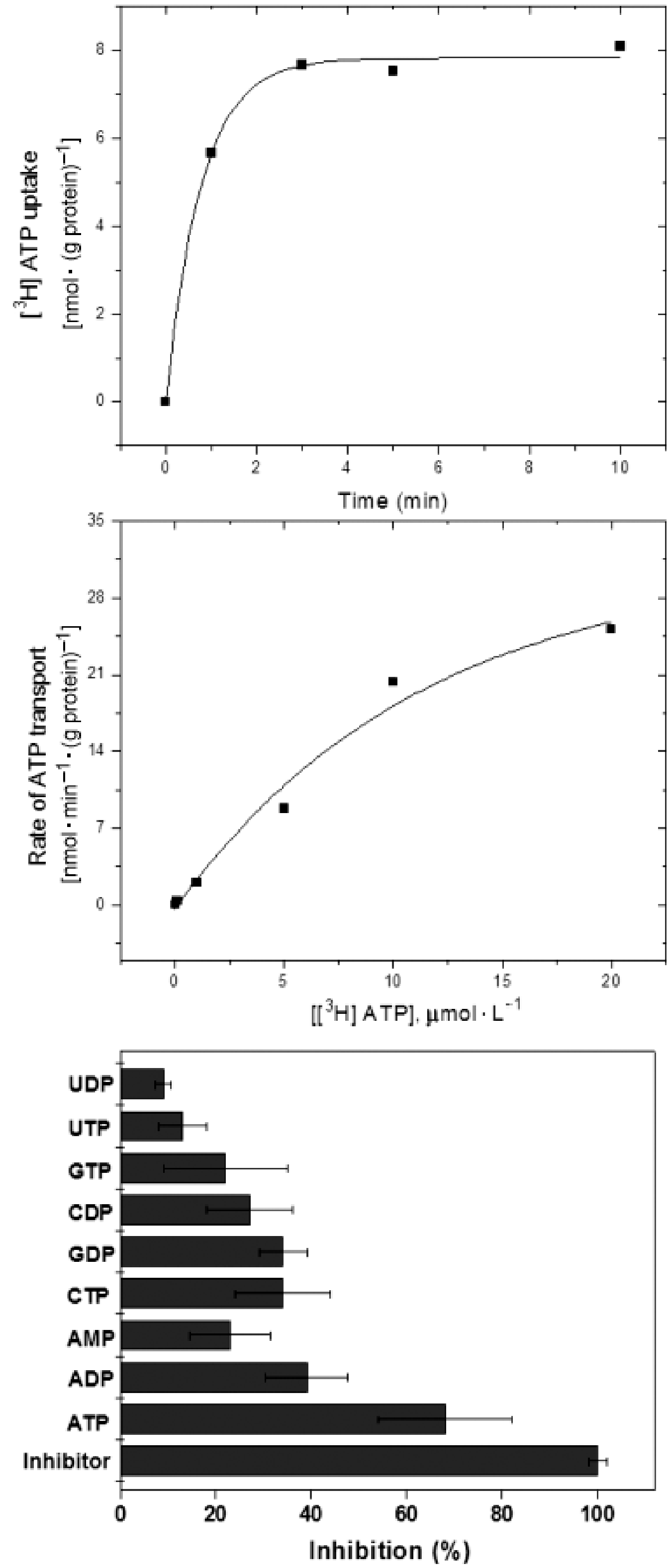

Fig. 2. Characterizatin of ATP-uptake by lipisome reconstituted recombinant ANT2. Upper panel: Time-course of ATP-uptake. Proteoliposomes containing ANT2 fusion protein were preloaded with 20 mmol·(L internal ATP)$^{-1}$. Transport was initiated by adding 5 µmol·(L [^{3}H] ATP)$^{-1}$ at the zero time point. Data points were calculated by subtracting the [^{3}H] ATP uptake observed in the presence of 2.0 mmol·(L pyridoxal 5′- phosphate)$^{-1}$ (inhibitor, non-specific background) from [^{3}H] ATP uptake levels obtained in the absence of inhibitor. Middle panel: Concentration dependence of [^{3}H] ATP uptake. Proteoliposomes containing ANT2 fusion protein were preloaded with 20 mmol·(L internal ATP)$^{-1}$. Rates were determined at each indicated [^{3}H] ATP concentration by fitting full 10 min time course curves to first order kinetics. The experiment was repeated twice, with each time point representing the average of six repetitions. Lower panel: Effect of external substrates on [^{3}H] ATP uptake. Proteoliposomes containing ANT2 fusion protein were preloaded with 20 mmol·(L internal ATP)$^{-1}$. Transport was initiated by the addition of 100 nmol·(L external [^{3}H] ATP)$^{-1}$ combined with 2.5 mmol·L^{-1} of each of the unlabelled substrates, at the zero time point. Transport was terminated after 10 min. Each of the data points are the average of three repetitions.

ver-stained SDS–PAGE and subjected to mass spectroscopic based peptide mass fingerprinting analysis, which confirmed the identity of both bands as ANT2. The presence of two ANT2 protein bands could represent incomplete delipidation by the detergent or protein modification events including either proteolytic digestion or, most likely, glycosylation.

To maintain solubility, cell lysis and subsequent Ni-NTA purification were carried out in the presence of Triton X-100 detergent. Directly after affinity purification, the ANT2 containing protein fraction was incorporated into liposomes consisting of L-α-phosphatedylcholine from egg yolk with 3% cholesterol and 20 mmol·(L internal ATP)$^{-1}$ (Bisaccia et al. 1985; Fiore et al. 1998). SDS–PAGE and Western blot analysis confirmed the presence of recombinant ANT2 fusion protein in the liposome samples (Fig. 1, bottom panels).

Kinetic parameters of recombinant ANT2-mediated ATP-transport in reconstituted liposomes

Uptake of [^{3}H]ATP by ANT2 liposomes was determined in the presence and absence of the ANT inhibitor, pyridoxal 5′-phosphate (Fiore et al. 1998). The uptake values observed for samples pre-treated with 2.0 mmol·(L inhibitor)$^{-1}$ were subtracted from the experimental uptake values observed in the absence of inhibitor. The time course yielded a curve indicating saturation of uptake (Fig. 2, top panel). In the case of 5 µmol·(L external [^{3}H] ATP)$^{-1}$, uptake reached approximately 8 nmol [^{3}H]ATP·(g protein)$^{-1}$. The presence of some background-labeled substrate was detected in the inhibitor-treated control samples. Comparison of these background [^{3}H]ATP values with [^{3}H]ATP values obtained for the uptake into liposomes containing no recombinant ANT2, confirmed the non-specific nature of the detected [^{3}H] ATP in control samples (data not shown). The presence of non-specific [^{3}H]ATP is most likely associated with diffusion or interaction of the substrate with the liposomes or the filter. Nonetheless, the differences observed in [^{3}H]ATP signals between inhibitor-treated and non-treated experimental samples clearly highlight recombinant ANT2's mediation of ATP-transport across the liposomal membrane.

Kinetic values were determined by the assessment of rates of ATP-transport at increasing concentrations of external [^{3}H]ATP (0.1–20 µmol·L^{-1}), with 20 mol·L^{-1} internal ATP. For each concentration, a full time course was completed and the resulting curve fit to first order kinetics to obtain the rate. Values for control samples pre-treated with 2 mmol·(L pyridoxal 5′-phosphate)$^{-1}$ (inhibitor) prior to [^{3}H]ATP addition were again subtracted from experimental values obtained in the absence of inhibitor. Increases in ATP-transport rates were observed with increasing concentrations of [^{3}H]ATP (Fig. 2, middle panel). The rate increased almost 20-fold [from ∼1 to >18 nmol·min^{-1}·(g protein)$^{-1}$] between 1 μmol·L^{-1} and 10 μmol·(L external [^{3}H] ATP)$^{-1}$. Further increasing the [^{3}H] ATP concentration to 20 μmol·L^{-1} led to a rate increase of only 6 nmol·min^{-1}·(g protein)$^{-1}$, highlighting a trend toward saturation. From this data, a K_m of 15 μmol·L^{-1} and a V_{max} of 45 nmol·min^{-1}·(g protein)$^{-1}$ were determined by Michaelis–Menten analysis using ENZFITTER software (Biosoft, Cambridge, UK). Each rate was determined twice, with each time point in the rate curve representing the average of 6 repetitions. Overall, these results demonstrate ATP translocation by ANT2.

[^{3}H] ATP transport by recombinant ANT2 in the presence of external substrates

To gain some insight into the substrate specificity of ANT2, proteoliposomes containing ANT2 fusion protein and preloaded with 20 mmol·(L internal ATP)$^{-1}$, were tested for uptake of 100 nmol·(L external [^{3}H]ATP)$^{-1}$ in the presence of 2.5 mmol·L^{-1} of external ATP, ADP, AMP, GTP, GDP, CTP, CDP, UTP, and UDP, respectively. As shown in Fig. 2 (bottom panel), transport was most sensitive to the presence of external ATP, which led to 62% inhibition of [^{3}H]ATP uptake compared with the pyridoxal 5′-phosphate inhibitor, set as 100% inhibition. Transport of labeled ATP was also inhibited, albeit to a lesser extent by exogenous ADP (39% inhibition), CTP (34% inhibition), and GDP (34% inhibition), indicating that these molecules are either taken up at low levels and (or) act as weaker inhibitors for ANT2. In contrast, [^{3}H]ATP uptake was not significantly affected by the presence of UTP, UDP, and AMP.

Discussion

The kinetic analyses reported herein, highlight the functionality of ANT2 as a specific ATP-translocator, modulating ATP uptake at rates similar to those observed for other ANTs. Specifically the value of 15 μmol·L^{-1} is within the range of K_m values previously documented for both native mitochondrial and plastidic ANT (3–30 μmol·L^{-1}), as well as other recombinant reconstituted ANT systems (10–70 μmol·L^{-1}) (Krämer and Klingenberg 1982; Bisaccia et al. 1985; Knirsch et al. 1989; Schünemann et al. 1993; Genchi et al. 1996; Tjaden et al. 1998; Millar and Heazlewood 2003; Leroch et al. 2008). However, it is important to note that the K_m and V_{max} values for ANT2 are reported here only as approximations of the actual kinetic parameter. Consideration of the Michaelis–Menten plot (Fig. 2) shows that while the rate of ATP-uptake began to plateau at 20 μmol·(L ATP)$^{-1}$ it has not reached complete saturation. Taking this aspect of the curve into consideration, we anticipate that the actual K_m of the reconstituted recombinantly produced ANT2 is likely a little higher than 15 μmol·L^{-1}, but probably still well within the range of values reported for other recombinant ANTs.

The reported binding specificities of ANT2 correlate with the specificities of homologous plant and mammalian systems reported previously. For example, the ANT from pea root plastids also displayed low affinity for UTP, UDP, and AMP (Schünemann et al. 1993; Genchi et al. 1996). In fact, in general, it has been shown that even though ANT substrate recognition is highly specific for ATP and ADP, some variations in transport selectivity do occur (Goto et al. 2002). Furthermore, several nucleotides and their analogues can bind to the ANT without being transported (Nury et al. 2006). For example, the ANT from bovine mitochondria binds (but does not transport) GDP and CTP (Brustovetsky and Klingenberg 1994). By contrast, the reconstituted ANT from maize mitochondria are capable of transporting GDP and GTP, although not as effectively as ATP (Genchi et al. 1996). These nucleotides were identified as competitive inhibitors for the reconstituted maize ANT. Mechanistic analyses of the interactions of targeted substrates on ANT2 are currently ongoing.

Overall, this study shows that *Arabidopsis thaliana* mitochondrial adenine nucleotide translocator 2 (ANT2) mediated ATP translocation. This demonstration of ANT2-mediated ATP uptake into proteoliposomes indicates that ANT2 is an ANT, confirming previous sequence based identification of the protein as a member of the ANT family. This work contributes to the expanding knowledge of the ANT family in *Arabidopsis* and opens up new prospects in further elucidating the physiological role of ANTs in plant cell metabolism.

Acknowledgements

We gratefully acknowledge Dr. Suzanne Abrams of the Plant Biotechnology Institute of the National Research Council of Canada for discussions, and Dr. Michelle Alting-Mees for critical reading of the manuscript. This work was funded by a National Research Council of Canada – Genomics Health Initiative grant to M.C.L. This manuscript represents NRCC No. 50145.

References

Bisaccia, F., Indiveri, C., and Palmieri, F. 1985. Purification of reconstitutively active alpha-oxoglutarate carrier from pig heart mitochondria. Biochim. Biophys. Acta, **810**(3): 362–369. doi:10.1016/0005-2728(85)90222-1. PMID:4063354.

Brustovetsky, N., and Klingenberg, M. 1994. The reconstituted ADP/ATP carrier can mediate H+ transport by free fatty acids, which is further stimulated by mersalyl. J. Biol. Chem. **269**(44): 27329–27336. PMID:7961643.

Fiore, C., Trézéguet, V., Le Saux, A., Roux, P., Schwimmer, C., Dianoux, A.C., Noel, F., Lauquin, G.J.-M., Brandolin, G., and Vignais, P.V. 1998. The mitochondrial ADP/ATP carrier: structural, physiological and pathological aspects. Biochimie, **80**(2): 137–150. doi:10.1016/S0300-9084(98)80020-5. PMID:9587671.

Genchi, G., Ponzone, C., Bisaccia, F., De Santis, A., Stefanizzi, L., and Palmieri, F. 1996. Purification and characterization of the reconstitutively active adenine nucleotide carrier from maize mitochondria. Plant Physiol. **112**(2): 845–851. doi:10.1104/pp.112.2.845. PMID:8883394.

Goto, S., Chuman, H., Majima, E., and Terada, H. 2002. How does the mitochondrial ADP/ATP carrier distinguish transportable ATP and ADP from untransportable AMP and GTP? Dynamic modeling of the recognition/translocation process in the major substrate binding region. Biochim. Biophys. Acta, **1589**(2): 203–218. doi:10.1016/S0167-4889(02)00173-8. PMID:12007795.

Klingenberg, M. 2008. The ADP and ATP transport in mitochondria and its carrier. Biochim. Biophys. Acta, **1778**(10): 1978–2021. doi:10.1016/j.bbamem.2008.04.011. PMID:18510943.

Knirsch, M., Gawaz, M.P., and Klingenberg, M. 1989. The isolation and reconstitution of the ADP/ATP carrier from wild-type *Saccharomyces cerevisiae*. Identification of primarily one type (AAC-2). FEBS Lett. **244**(2): 427–432. doi:10.1016/0014-5793(89)80577-0.

Krämer, R., and Klingenberg, M. 1982. Electrophoretic control of reconstituted adenine nucleotide translocation. Biochemistry, **21**(5): 1082–1089. doi:10.1021/bi00534a040. PMID:6280754.

Kunji, E.R.S. 2004. The role and structure of mitochondrial carriers. FEBS Lett. **564**(3): 239–244. doi:10.1016/S0014-5793(04)00242-X. PMID:15111103.

Leroch, M., Neuhaus, S., Kirchberger, S., Zimmermann, S., Melzer, M., Gerhold, J., and Tjaden, J. 2008. Identification of a novel adenine nucleotide transporter in the endoplasmatic reticulum of *Arabidopsis*. Plant Cell, **20**(2): 438–453. doi:10.1105/tpc.107.057554.

Millar, A.H., and Heazlewood, J.L. 2003. Genomic and proteomic analysis of mitochondrial carrier proteins in *Arabidopsis*. Plant Physiol. **131**(2): 443–453. doi:10.1104/pp.009985. PMID:12586869.

Möhlmann, T., Tjaden, J., Schwöppe, C., Winkler, H.H., Kampfenkel, K., and Neuhaus, H.E. 1998. Occurrence of two plastidic ATP/ADP transporters in *Arabidopsis thaliana* L.: molecular characterisation and comparative structural analysis of similar ATP/ADP translocators from plastids and *Rickettsia prowazekii*. Eur. J. Biochem. **252**(3): 353–359. doi:10.1046/j.1432-1327.1998.2520353.x. PMID:9546649.

Mozo, T., Fischer, K., Flügge, U.I., and Schmitz, U.K. 1995. The N-terminal extension of the ADP/ATP translocator is not involved in targeting to plant mitochondria *in vivo*. Plant J. **7**(6): 1015–1020. doi:10.1046/j.1365-313X.1995.07061015.x. PMID:7599644.

Neuhaus, H.E., Thom, E., Möhlmann, T., Steup, M., and Kampfenkel, K. 1997. Characterization of a novel eukaryotic ATP/ADP translocator located in the plastid envelope of *Arabidopsis thaliana* L. Plant J. **11**(1): 73–82. doi:10.1046/j.1365-313X.1997.11010073.x. PMID:9025303.

Nury, H., Dahout-Gonzalez, C., Trezeguet, V., Lauquin, G.J.M., Brandolin, G., and Pebay-Peyroula, E. 2006. Relationshios between structure and function of the mitochondrial ADP/ATP carrier. Annu. Rev. Biochem. **75**(1): 713–741. doi:10.1146/annurev.biochem.75.103004.142747.

Palmieri, L., Santoro, A., Carrari, F., Blanco, E., Nunes-Nesi, A., Arrigoni, R., Genchi, F., Fernie, A.R., and Palmieri, F. 2008. Identification and characterization of ADNT1, a novel mitochondrial adenine nucleotide transporter from *Arabidopsis*. Plant Physiol. **148**(4): 1797–1808. doi:10.1104/pp.108.130310. PMID:18923018.

Picault, N., Hodges, M., Palmieri, L., and Palmieri, F. 2004. The growing family of mitochondrial carriers in *Arabidopsis*. Trends Plant Sci. **9**(3): 138–146. doi:10.1016/j.tplants.2004.01.007. PMID:15003237.

Schünemann, D., Borchert, S., Flügge, U.-I., and Heldt, H.W. 1993. ADP/ATP translocator from pea root plastids. Comparison with translocators from spinach chloroplasts and pea leaf mitochondria. Plant Physiol. **103**(1): 131–137. PMID:12231920.

Schuster, W., Kloska, S., and Brennicke, A. 1993. An adenine nucleotide translocator gene from *Arabidopsis thaliana*. Biochim. Biophys. Acta, **1172**(1-2): 205–208. PMID:8439563.

Tjaden, J., Schwöppe, C., Möhlmann, T., Quick, P.W., and Neuhaus, H.E. 1998. Expression of a plastidic ATP/ADP transporter gene in *Escherichia coli* leads to a functional adenine nucleotide transport system in the bacterial cytoplasmic membrane. J. Biol. Chem. **273**(16): 9630–9636. doi:10.1074/jbc.273.16.9630. PMID:9545295.

Trentmann, O., Decker, C., Winkler, H.H., and Neuhaus, H.E. 2000. Charged amino-acid residues in transmembrane domains of the plastidic ATP/ADP transporter from *Arabidopsis* are important for transport efficiency, substrate specificity, and counter exchange properties. FEBS Lett. **267**: 4098–4105.